Physica E: Low-dimensional Systems and Nanostructures 112 (2019) 19–25

Contents lists available at ScienceDirect

Physica E: Low-dimensional Systems and Nanostructures

journal homepage: www.elsevier.com/locate/physe

Nucleation of gold nanoclusters in PMMA during energetic plasma deposition: A molecular dynamics and tfMC-Monte Carlo study

F.S. Teixeira*, M.C. Salvadori

Institute of Physics, University of São Paulo, C.P. 66318, CEP 05315-970, São Paulo, S.P., Brazil

ARTICLE INFO

Keywords:
Gold nanoparticles
Nucleation
FCVA
tfMC Monte Carlo

ABSTRACT

We have explored the nucleation of gold nanoclusters in PMMA (Poly[methyl methacrylate]) using theoretical simulations. The nanoclusters are formed from energetic condensation of gold ions in the polymer from the very first deposition pulse. Three gold ion energy values are considered (50 eV, 100 eV and 150 eV). The influence of ion energy on sputtering, nucleation, diffusion and depth profile is discussed. For energetic plasma deposition techniques, including Filtered Cathodic Vacuum Arc (FCVA) deposition, the arrival of ions to the system can be considered as rare events. Therefore, to access a complete description of the nucleation process, Molecular Dynamics simulation is combined with time stamped force bias Monte-Carlo (tfMC) for the first pulse of deposition.

1. Introduction

Gold nanoclusters are of interest to the scientific community because of potential applications in a number of fields including cancer therapy, drug delivery, biosensing, electronics and nanophotonics [1]. In particular, plasmon resonance in gold particles [2] is an important property with a variety of applications such as chemical sensing by SERS (Surface Enhanced Raman Spectroscopy), cell imaging, catalysis, non-linear optics and photoconversion. Gold nanoparticles are also advantageous because of their high chemical and physical stability and their biocompatibility.

Filtered Cathodic Vacuum Arc (FCVA) deposition [3] is a plasma deposition technique widely used for the formation of micro- and nanostructured thin films by energetic condensation. As described by Anders [4–6], energetic condensation is a deposition process in which a significant fraction of the condensing species are deposited at hyperthermal energies, which in practice implies deposition energy values greater than about 10 eV. Energetic condensation leads to surface and subsurface processes that are activated or enabled by the energy of the depositing particles. Salvadori and coworkers have used FCVA deposition techniques for the formation of gold nanoclusters embedded in PMMA, with primary interest in the electrical and optical properties of the synthesized material [8–12]. The characteristic deposition energy for gold using the FCVA technique is ~50 eV [7], which is adequate for the formation of nanoparticles below the surface of the substrate. However, details of the formation process involved have not previously been investigated.

In the FCVA deposition approach, energetic metal ions (energy typically 20–150 eV depending on the ion species) are formed by a vacuum arc discharge and magnetically guided to the substrate surface [7]. The characteristic ion energy for each specific element is an inherent feature of the vacuum arc discharge, but a biased mesh technique can be used to further control the ion energy [12]. Deposition is carried out in a repetitively pulsed mode, with pulse width typically about 5 msec and repetition rate typically about 1 Hz. There are some advantages of this approach over sputtering and other physical deposition techniques, including fine control of the deposition dose; each deposition pulse typically deposits a very small dose (~10^{14} atoms/cm^2), corresponding roughly to just one tenth of a monolayer. However, for this technique, gold impingement on the surface is a rare event.

Molecular Dynamics (MD) is a powerful computational tool in which the dynamic behavior of a system of particles (atoms, molecules or macromolecules) is determined by numerically solving Newton's equations of motion. Once the interaction potentials between the particles are known, the temporal evolution of phase space configurations (positions and momenta) can be determined. The microscopic details of the system can be accessed, as well as several macroscopic properties by

* Corresponding author.
E-mail address: nandast@if.usp.br (F.S. Teixeira).

https://doi.org/10.1016/j.physe.2019.03.026
Received 21 December 2018; Received in revised form 27 February 2019; Accepted 25 March 2019
Available online 29 March 2019
1386-9477/

using a statistical mechanics approach. Although the concept of statistical system ($\sim 10^{23}$ particles) is adopted to a very good approximation, due to computational limitations the physical dimensions of the system are limited to $\sim 10^4$ particles. Similarly the evolution time that can be reached is limited to a range from picoseconds (ps) to nanoseconds (ns). Even so, MD provides an invaluable technique for studying a broad range of problems in physics, chemistry, materials science and biological systems [13]. The choice of intra and inter interaction potentials constitutes a critical stage in a correct description of the system. The interaction potentials determine the forces that act on each particle and consequently the correct evolution of the system dynamics.

A problem arises when different equilibrium states or some rare events can occur in a larger time window, as when there are longer thermal relaxation processes. Two possible solutions are (1) to use other simulation techniques rather than MD, such as a completely stochastic Kinetic Monte Carlo approach [14], or (2) to use methods for extending the MD timescale, such as accelerated molecular dynamics methods or a combination/alternation of MD with force-bias Monte Carlo methods (stochastic but including deterministic forces). Kinetic Monte Carlo techniques have been used to simulate very long timescale processes such as thin film deposition and diffusion processes. However, all relevant processes and the associated rate constants have to be known in advance, which can be a very difficult task. Several methods exist for molecular dynamics acceleration, such as Parallel Replica Dynamics, Hyperdynamics and Temperature Accelerated Dynamics, (TAD). In parallel replica dynamics [15], many replicas are run and the accepted transition is the first escape found in any of the replicas. The escape time is then the sum of MD times on all replicas up to the instant of that escape of a state. In hyperdynamics [16] one has to define a bias potential to be added to the normal potential to make escape barriers lower. Defining an optimal bias potential is not a trivial task and another developments help on that, such as bond boost [17] and Collective Variable Hyperdynamics (CVHD) [18]. Both those acceleration methods (Parallel Replica Dynamics and Hyperdynamics) relies on the definition and identification of a potential surface with deep energy minima, which are not a feature of the system studied in this work.

To extend the MD timescale, a TAD approach can also be used [19]. This technique simulates the system at higher temperature so as to increase the event rate, but only accepting events that would occur at the temperature of interest but over a longer timescale. A disadvantage of TAD in the context of the work presented here is thermal dilation of the system; this is quite relevant to polymeric systems and can lead to very imprecise simulation.

Abraham et al. [20] showed an interesting approach in which there is a computational gain by considering the polymer a continuous background driven by Langevin dynamics instead of a particle-based medium. However, they considered a constant flux of gold arriving on the surface instead of rare deposition events.

Another means for extending the MD timescale is to combine it with force-bias Monte Carlo methods [21–23], in special time stamped force-bias Monte Carlo (tfMC Monte Carlo). Although stochastic in essence, the interaction potential between particles is accounted (force bias) and a timescale can be associated with the evolution of particle positions, providing some insight into the dynamics. However, there are divergences about the time scale [23], which suggests that it can reach longer average times than previously suggested [21], which is actually an advantage. The technique has been used to simulate surface diffusion and defected graphene healing [21]. In a physical deposition process, the collision of an atom with the surface triggers fast processes, but the deposition itself is a rare event, i.e. there is a long time between events. Thus the atom impingement and its consequences to the target can be evaluated by MD, while the evolution of the long thermal relaxation can be followed by tfMC. This approach was used in this work.

2. Method

The LAMMPS (Large-scale Atomic/Molecular Massively Parallel Simulator) Molecular Dynamics simulator [24,25] was used to run both MD simulations and tfMC (time-stamped force-bias Monte Carlo) simulations. LAMMPS is a classical molecular dynamics code that can model atomic systems through coarse-grained systems using several kinds of force fields. There is also an implemented algorithm (*fix tfmc* command) that performs tfMC, as described by Mees and Bal [21,23]. Further, *chain.py* was used, an available algorithm [24] that creates bead-spring chains of polymers for LAMMPS input. The set-up of the simulations is described in detail in the following.

2.1. Potentials and preparation of the PMMA substrate

PMMA, or poly(methyl methacrylate), is an acrilic polymer whose monomer formula is $(C_5O_2H_8)_n$. An explicit model is not necessary and would render the simulation unfeasible because of the very large number of interacting particles. A coarse-graining approach [26] was adopted. The PMMA model used is from the literature [27–29] and includes representation of the entire monomer $C_5O_2H_8$ (mass = 100 u) by a single particle. The polymer is then represented by a set of chains, where each chain is formed by a set of connected monomers (or particles). Monomers in the same chain interact attractively through a FENE (Finite Extensible Non-linear Elastic) potential and repulsively through the Lennard Jones potential. Monomers in different chains interact uniquely through the Lennard Jones potential.

The FENE potential is given by Refs. [26–29].

$$U_{FENE}(r) = -\frac{k}{2}R_0^2 \ln\left[1 - \left(\frac{r}{R_0}\right)^2\right] \quad (1)$$

where k is the bond stiffness and R_0 the equilibrium bond length. The parameter values used were $k = 0.08\ \mathrm{eV/Å^2}$ and $R_0 = 7.5$ Å. Note that these values are not in Lennard Jones units, but in metal units [24].

Both PMMA monomers (of different chains) and Au particles interact by pair-wise Lennard Jones potentials [13,29]. The very well known intermolecular 12-6 Lennard Jones Potential is given by

$$U_{LJ}(r) = 4\varepsilon\left[\left(\frac{\sigma}{r}\right)^{12} - \left(\frac{\sigma}{r}\right)^{6}\right] = 4\varepsilon\left[\left(\frac{Rmin}{r}\right)^{12} - 2\left(\frac{Rmin}{r}\right)^{6}\right] \quad (2)$$

where $Rmin = \sqrt[6]{2}\sigma$ is the distance for which the potential reaches its minimum, ε is the potential well and σ is the distance for which the potential between particles is zero.

Table 1 shows the Lennard Jones parameters for Au-Au [29] and monomer-monomer [26–28] interactions. Au-monomer interactions are calculated using geometric combination rule [24,29].

Note that the possibility of using Lennard Jones potentials for all the

Table 1
12-6 Lennard Jones potential parameters used for Au-Au interactions and for monomer-monomer interactions. The cut radius used for the simulations was 2.5σ.

	σ [Å][a]	ε [eV][a]
Au-Au	5.160	0.0700
monomer-monomer	2.629	0.2294

[a] Note that values are not in Lennard Jones units, but in metal units [24].

particles in the system, including Au-Au [29], is of great advantage in terms of computational cost. For metals, many-body embedded atomic models (EAM) are often used, but Heinz [29] shows accurate simulations involving mechanical properties and nanometer-scale surface/interface energy properties for several fcc metals. The author claims that the LJ parameters developed can be used in simulations combining metal with organic, inorganic and biological structures.

For fabrication of PMMA a set of 3000 monomers was created, divided into 50 chains, each formed by 60 monomers. A mass of 100 u was associated with each monomer. Periodic boundary conditions for x and y directions were used. Periodic boundary conditions for the z-axis were broken to create an upper polymer surface and a bottom edge (fixed to imitate an infinite substrate). The system timestep was set to 0.0025 ps. The system was then heated from 300 K to 1000 K for 2.5 ns, equilibrated at 1000 K during 75 ns, quenched down to 300 K in 250 ns and equilibrated for 125 ns. With proper adjustments, the final system had dimensions 50 Å × 50 Å × 180 Å and calculated density $\rho = 1.13\ g/cm^3$, a value consistent with a PMMA coarse-grained model [26].

2.2. Simulation box and simulation settings

A schematic drawing of the simulation box is shown in Fig. 1. The fixed layer, thermal bath and active layer are different regions of the polymer; that is, these regions are composed of monomers. For the fixed layer (10 Å) the particles are not time integrated, remaining still and imitating an infinite substrate. The particles of the thermal bath (50 Å) are time integrated and their temperature is controlled by a Langevin thermostat.

The particles of the active layer (120 Å) are time integrated with no

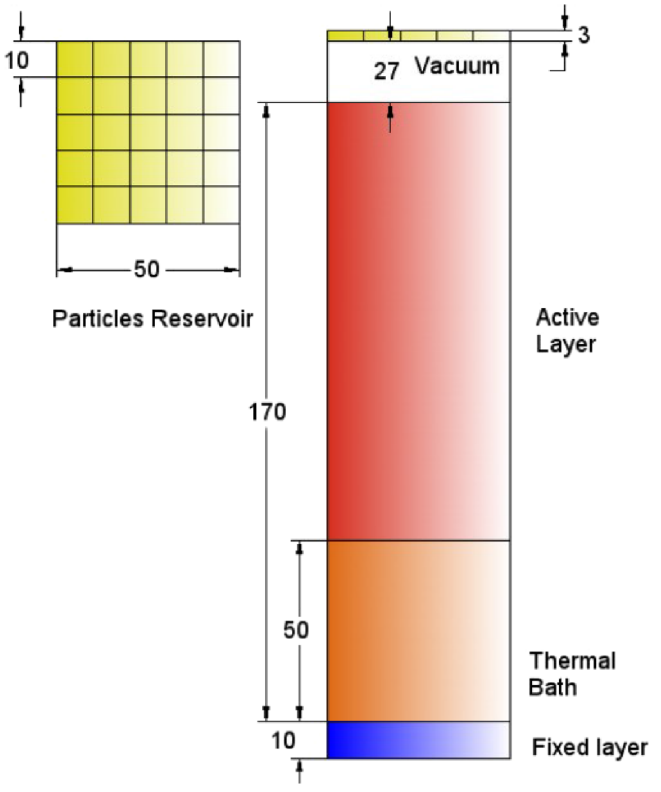

Fig. 1. Simulation box for energetic deposition of Au on PMMA. Units are in angstroms.

temperature control. Above the vacuum layer (with no particles), there is a layer that works as a Au atom reservoir. This layer has a lateral area of 50 Å × 50 Å and is divided into 25 regions of 10 Å × 10 Å. For each deposition event, two atoms are randomly drawn from two of these 25 regions. The velocity v_z of each atom is associated with its energy. The values of v_x and v_y are zero, which corresponds to normal incidence with respect to the polymer surface. Three energy values were used for deposition: 50 eV, 100 eV and 150 eV, corresponding to 70 Å/ps, 99 Å/ps and 121 Å/ps, respectively. We assume here that the Au particles are neutral. The deposition is maintained for 2000 steps. For each deposition, there is momentum transfer that increases the temperature of the active layer, which is dissipated by the thermal bath layer. The timestep was set to 0.0025 ps.

To design the Langevin thermostat that controls the thermal bath, we take a thermal capacity $k = 0.2$ W/m.K and specific heat $c = 146$ J/kg.K for PMMA [30]. Then the heat flux is given by

$$\Delta Q/\Delta t = (kA\ \Delta T)/L \tag{3}$$

where A is the area of the active layer (50 Å × 50 Å), L is its thickness (120 Å) and ΔT is the temperature variation.

The amount of heat that has to be dissipated is

$$\Delta Q = mc\Delta T = \rho V \Delta T \tag{4}$$

where ρ is the PMMA density and V is the volume of the active layer.

Combining Eqs. (3) and (4), we find that according to the PMMA thermal parameters, the heat of the active layer must be dissipated in ~1 ns. Throughout some simulations, it was found that the correct damping parameter of the Langevin thermostat for this dissipation time is 0.1 ps. After the deposition event, MD was run for 2.5 ns.

As the MD time scale runs from picoseconds to nanoseconds, as above, it is important to extend this time limit to reach other equilibrium situations. The tfMC technique [23,24] does this task based on a probabilistic atomic movement distribution (including deterministic forces given by the interaction potentials). The value of Δ must be chosen to be 5%–10% of the typical nearest neighbor distance in order to not violate the detailed balance [22,23]. For PMMA, from the radial distribution function, the nearest neighbor distance is 5 Å [26], so Δ was chosen as Δ = 0.25 Å.

The deposition rate is 1 Hz, corresponding to one plasma pulse per second, but in this work the goal is to understand what happens in the *first* pulse. The pulse duration is 5 ms. A reasonable dose per pulse is $1.0 \times 10^{14} cm^{-2}$. This corresponds to approximately 26 atoms arriving over 25 nm^2 during the 5 ms period. Considering the incidence of two atoms (that we define here as a deposition event) and the total of 26 atoms, we can calculate that the time between events is 5000 μs/13 = 384 μs.

As already pointed out in "Introduction" section, the exactly tfMC timescale cannot be calculated. However, the primary interest of the simulation is to capture a system configuration that is beyond the MD timescale, which can be of complete agglomeration, for instance. We can assume that the agglomeration process happens in a characteristic time for the gold/PMMA system. To probe this time, auxiliary short simulations was done with 13 deposition events of 2 atoms each. The energy of each incident atom was 100 eV. After each deposition event, 2×10^6 MD steps were performed. The resulting system was then submitted to 7×10^8 tfMC steps. Also, this auxiliary simulation was done to show the resulting configuration of the system with MD technique alone (before 7×10^8 tfMC steps).

Another auxiliary set of simulations were done in order to determine the diffusion coefficient of one gold atom ($na = 1$) and of gold clusters as a function of the number of atoms na ($2 \leq na \leq 7$). We simulated two cases, first one particle inside the polymer and second two

particles inside the polymer to account interaction between particles. For the first case, the atom or the cluster was put in the middle of the polymer slab (position x = y = 25 Å and z = 100 Å) and the system was minimized. Equilibration of 5×10^6 steps was done and then a production simulation of 5×10^6 steps was done. The timestep was 0.0025 ps. For the second case, two atoms or two clusters were put inside the polymer slab at positions x = y = 25 Å and z_1 = 25 Å and z_2 = 125 Å.

For the main simulations, the sequence summary for each deposition event was: (1) deposition of 2 atoms drawn randomly from the atom reservoir with energy for 5 ps; (2) Molecular Dynamics simulation for 2.5 ns; (3) 10^8 steps of tf Monte Carlo simulation. We have calculated the diffusion coefficients for the first deposition event (with 2 atoms) for each energy as a function of the time for the first 10 ns.

The simulations were run at the High Performance Computing Center of the University of Sao Paulo, using Lince cluster (32 servers, each one with 16 Intel(R) Xeon(R) E5-2680 rv0 @ 2.70 GHz) physical cores. Three independent simulations were done for each energy. Each main simulation was done in about 330 h.

3. Results and discussion

The result of the auxiliary simulation done in order to estimate the characteristic agglomeration time of the Au/PMMA, before the final tfMC steps, was a system composed of isolated atoms and tiny particles as can be seen in Fig. 2(a). After 1×10^8 tfMC steps there was a complete agglomeration into larger clusters of about 3–7 atoms, see Fig. 2(b). After 7×10^8 tfMC steps the system configuration does not change appreciably, showing that clusters with more than 3 atoms have very low mobility. In this way, 10^8 tfMC timesteps were adopted as sufficient for the main simulations.

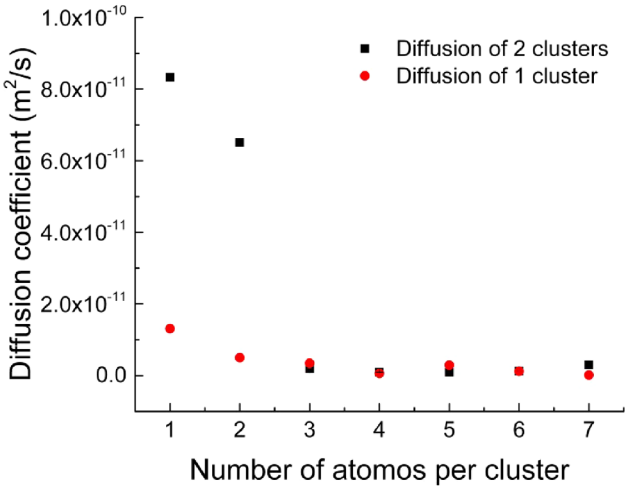

Fig. 3. Single atom and cluster diffusion coefficients as a function of the number of atoms for 1 particle inside the polymer (circles) and 2 particles inside the polymer (squares).

Fig. 3 shows the single atom and cluster diffusion coefficient as a function of the number of atoms. We can see that for clusters with more than 3 atoms, the mobility decreases, reaching values of the order of $(1 \pm 0.01) \times 10^{-12}\ m^2/s$.

For the regular simulations, the active layer reached temperature

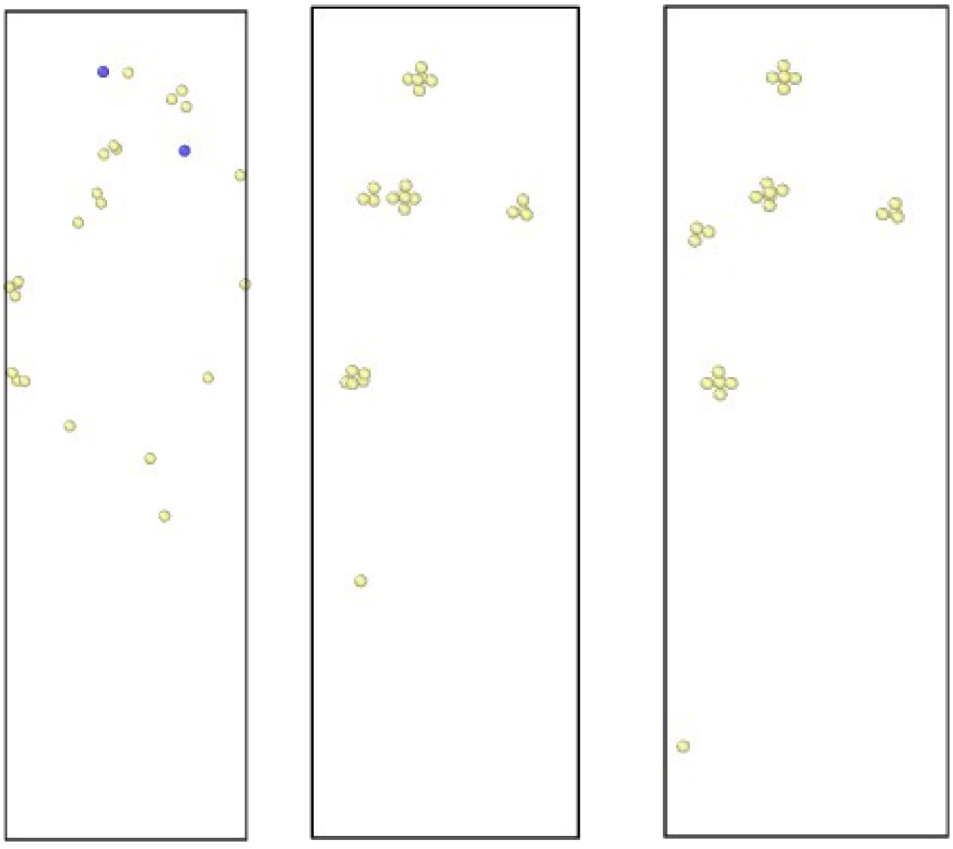

Fig. 2. a) Result of a simulation of 13 deposition events of 2 atoms each. After each deposition, 2×10^6 MD steps were made. a-) System configuration after MD simulation, showing several nucleation sites b-) System configuration after 1×10^8 tfMC steps showing agglomeration c-) System configuration after 7×10^8 steps, showing the limited mobility of the clusters. The polymer monomers were omitted for clarity. The simulation box lateral dimension is 5 nm.

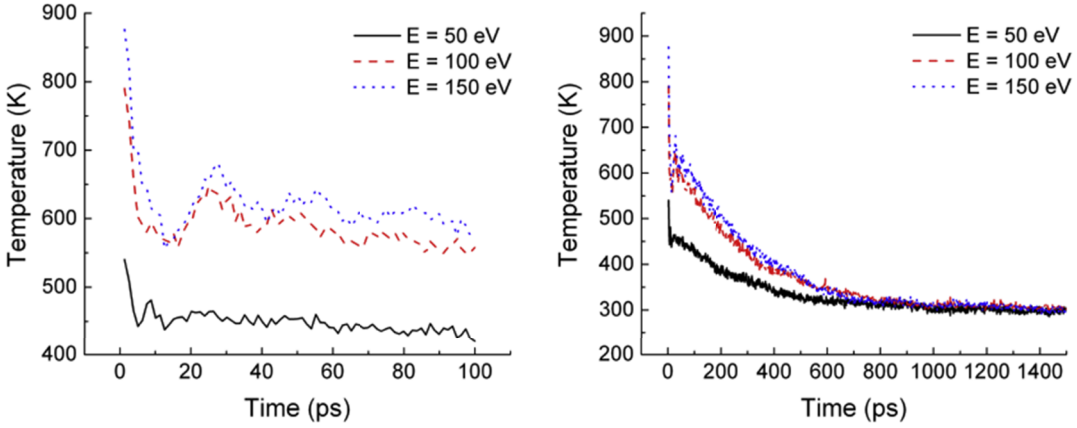

Fig. 4. Representative graphs showing (a) Temperature behavior just after deposition, and (b) Dissipation over ~1 ns.

peaks of ~540 K, ~790 K and ~876 K for 50 eV, 100 eV and 150 eV kinetic energy, respectively, as shown in Fig. 4(a). Fig. 4(b) shows the temperature dissipation in approximately 1 ns. The depth profile is essentially the same for the three energies used, at least for the first pulse. The sputtering and the number of broken bonds increases with energy, as can be seen from Table 2. Thus we can suggest that for more pulses, the depth profile can be different for different energies.

Fig. 5 shows the diffusion coefficients for the first deposition event (with 2 atoms) for each energy as a function of the time for the first 10 ns. We can see that there is a difference in diffusion coefficient for each initial deposition energy. Taking the last 1 ns, the average diffusion coefficient for each energy is $(1.02 \pm 0.04) \times 10^{-9}\,m^2/s$ for 50 eV, $(1.22 \pm 0.05) \times 10^{-9}\,m^2/s$ for 100 eV and $(2.03 \pm 0.08) \times 10^{-9}\,m^2/s$ for 150 eV. Fig. 6 shows the dynamics of Au atom momenta transfer to the polymer surface monomers for the first deposition event, where the role of crescent energy is clear.

Table 2
Number of polymer broken bonds and sputtered atoms as a function of atom energy.

Deposition energy	Number of broken bonds	Number of sputtered atoms
50 eV	0	< 1
100 eV	~3	~3
150 eV	~87	~93

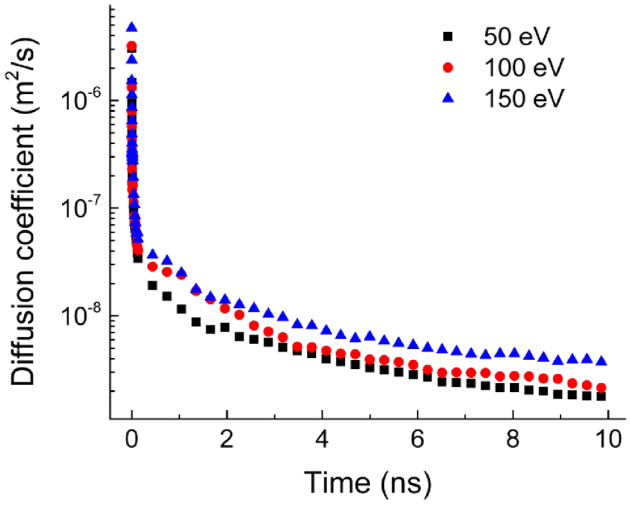

Fig. 5. Diffusion coefficients as a function of the initial deposition energy.

Au particles completely nucleate inside the polymer on the very first pulse; see Fig. 7. For every deposition event during tfMC simulation, the gold atoms diffuse as a Brownian motion. When the distance between two gold particles or a gold particle and an existing cluster is such that there is an attraction potential, corresponding to $2.5\sigma = 2.5 \times 5.160^{-}13$ Å (see Table 1), agglomeration occurs. The stronger interaction potential for Au-Au than for Au-monomer particles together with the polymer mobility is sufficient to allow the nucleation of gold during the first pulse. The particles have diameter of ~1 nm.

In fact, by Fig. 2, it is clear that agglomeration also occurs in the MD simulation. However, we see several nucleation sites been formed. When these nucleation sites are formed by some atoms (≥3), their mobility decreases. Using tfMC, the behavior is quite different: for the size of the simulation box chosen, one nucleation site is established and, for subsequent deposition events, there is sufficient time (experimentally 1s) for the new isolated atoms (with increased mobility) to join the site.

4. Summary and conclusions

We have considered the deposition of gold on PMMA polymer with three different deposition energies (50 eV, 100 eV and 150 eV). For all three energies, shallow implantation occurs and the depth profiles are comparable for the first pulse. However, the number of polymer broken bonds and sputtered atoms increases with energy, which probably influences the depth profile for subsequent deposition pulses. The use of Lennard Jones pairwise potentials for gold and monomers was essential to make the simulations feasible due to the large computation time requirements. The use of tfMC was essential to reach sufficient time to show that total agglomeration occurs for every deposition event, culminating in complete nucleation for the first pulse of 1.0×10^{14} atoms/cm^2 for FCVA deposition, a very original result.

Acknowledgments

This work was supported by the Fundação de Amparo a Pesquisa do Estado de São Paulo (FAPESP), the Conselho Nacional de Desenvolvimento Científico e Tecnológico (CNPq) grant number 304407/2013-5. We would like to thank Ettore Enrico Delfino Ligorio

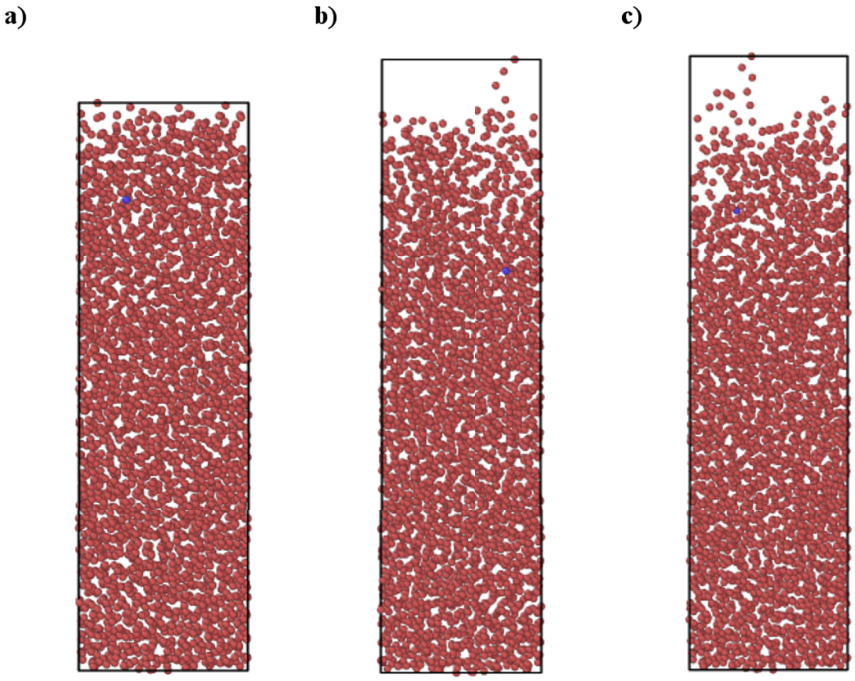

Fig. 6. Representative snapshots of momentum exchange between energetic gold atoms and polymer for (a) 50 eV, (b) 100 eV and (c) 150 eV. The simulation box lateral dimension is 5 nm.

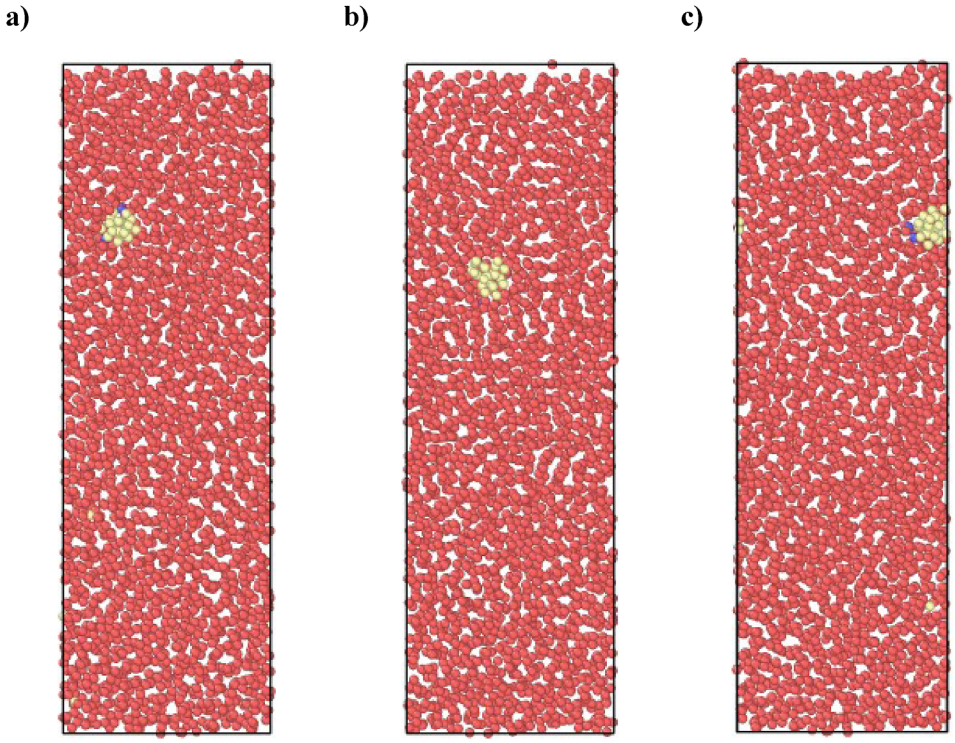

Fig. 7. Nanoclusters formation for energies of (a) 50 eV, (b) 100 eV and (c) 150 eV. Polymer monomers are represented by red spheres and gold particles by yellow and blue spheres (atoms from the last deposition). The nanoparticle depth is (a) ~ 4 nm, (b) ~ 5 nm and (c) ~ 4 nm The simulation box lateral dimension is 5 nm. (For interpretation of the references to colour in this figure legend, the reader is referred to the Web version of this article.)

and Francisco Ribacionka from HPC-USP (http://www.usp.br/hpc/) for computational support. We thank also LAMMPS developers, Prof. Caetano Miranda of the Institute of Physics (USP), Dr. Wagner Wlysses Araújo of the Institute of Physics (USP) and Prof. Antonio Rodrigues da Cunha of Universidade Federal do Maranhão for valuable suggestions.

References

[1] C. Louis, O. Pluchery, Gold Nanoparticles for Physics, Chemistry and Biology, Imperial College Press, London, 2012.
[2] V. Amendola, R. Pilot, M. Frasconi, O.M. Maragò, M.A. Iatì, J. Phys. Condens. Matter 29 (2017) 203002.
[3] I.G. Brown, Annual Review of Materials Science vol. 28, Annual Reviews, Palo Alto, CA, 1998.
[4] A. Anders, Cathodic Arcs from Fractal Spots to Energetic Condensation, Springer, 2008.
[5] A. Anders, J. Phys. D Appl. Phys. 40 (2007) 2272–2284.
[6] A. Anders, Vacuum 67 (2002) 673–686.
[7] A. Anders, G.Y. Yushkov, J. Appl. Phys. 91 (8) (2002).
[8] M.C. Salvadori, M. Cattani, F.S. Teixeira, I.G. Brown, Appl. Phys. Lett. 93 (2008) 073102.
[9] F.S. Teixeira, M.C. Salvadori, M. Cattani, S.M. Carneiro, I.G. Brown, J. Vac. Sci.

Technol. B 27 (5) (2009) 2242–2247.
[10] J. Ferreira, F.S. Teixeira, A.R. Zanatta, M.C. Salvadori, R. Gordon, O.N. Oliveira, Phys. Chem. Chem. Phys. 14 (6) (2012) 2050–2055.
[11] F.S. Teixeira, M.C. Salvadori, M. Cattani, S.M. Carneiro, I.G. Brown, J. Vac. Sci. Technol. B 27 (5) (2009) 2242–2247.
[12] A. Moafi, D.W.M. Lau, A.Z. Sadek, J.G. Partridge, D.R. Mackenzie, D.G. McCulloch, J. Appl. Phys. 109 (2011) 073309.
[13] M.E. Tuckerman, Statistical Mechanics: Theory and Molecular Simulation, Oxford University Press, New York, 2010.
[14] A.F. Voter, Introduction to the kinetic Monte Carlo method, in: K.E. Sickafus, E.A. Kotomin, B.P. Uberuaga (Eds.), Radiation Effects in Solids. NATO Science Series, vol. 235, Springer, Dordrecht, 2007.
[15] D. Perez, B.P. Uberuaga, A.F. Voter, Comput. Mater. Sci. 100 (2015) 90–103.
[16] S.Y. Kim, D. Perez, A.F. Voter, J. Chem. Phys. 139 (2013) 144110.
[17] K.A. Fichthorn, S. Mubin, Comput. Mater. Sci. 100 (2015) 104–110.
[18] K.M. Bal, E. Neyts, J. Chem. Theory Comput. 11 (2015) 4545–4554.
[19] M.R. Sorensen, A.F. Voter, J. Chem. Phys. 112 (21) (2000) 9599.
[20] J.W. Abraham, T. Strunskus, F. Faupel, M. Bonitz, J. Appl. Phys. 119 (2016) 185301.
[21] M.J. Mees, G. Pourtois, E.C. Neyts, B.J. Thijsse, A. Stesmans, Phys. Rev. B 85 (2012) 134301.
[22] E.C. Neyts, B.J. Thijsse, M.J. Mees, K.M. Bal, G. Pourtois, J. Chem. Theor. Comput. 8 (2012) 1865–1869.
[23] K.M. Bal, E.C. Neyts, J. Chem. Phys. 141 (2014) 204104.
[24] S. Plimpton, Fast parallel algorithms for short-range molecular dynamics, J. Comput. Phys. 117 (1995) 1–19.
[25] Website, http://lammps.sandia.gov.
[26] B. Schnell, Etude par simulation numérique de la transition vitreuse et de l'état vitreux de polymères denses amorphes: propriétés mécaniques et phénomène de cavitation PhD Thesis in Polymer Physics Strasbourg (France): thesis UdS, (2006).
[27] M. Solar, H. Meyer, C. Gauthier, O. Benzerara, H. Pelletier, R. Schirrer, J. Baschnagel, J. Phys. D Appl. Phys. 43 (2010) 455406.
[28] M. Solar, H. Meyer, C. Gauthier, O. Benzerara, R. Schirrer, J. Baschnagel, Wear 271 (2011) 2751–2758.
[29] H. Heinz, R.A. Vaia, B.L. Farmer, R.R. Naik, J. Phys. Chem. C 112 (2008) 17281–17290.
[30] Website, www.mit.edu/~6.777/matprops/pmma.htm.